

## Chemistry of Iron Oxophlorins. 3. Reversible, One-Electron Oxidation of the Iron(III) Octaethyloxophlorin Dimer

Alan L. Balch,<sup>\*,†</sup> Lechosław Latos-Grażyński,<sup>‡</sup> and Tamara N. St. Claire<sup>†</sup>

Department of Chemistry, University of California, Davis, California 95616, and University of Wrocław, Wrocław, Poland

Received December 9, 1994<sup>®</sup>

The oxidative behavior of the dimeric octaethyloxophlorin (OEPOH<sub>3</sub>) complex, {Fe<sup>III</sup>(OEPO)}<sub>2</sub>, **1**, has been studied in regard to its relevance toward heme catabolism and the effects of  $\pi$ - $\pi$  overlap as seen in the chlorophyll special pair. Electrochemical studies show that {Fe<sup>III</sup>(OEPO)}<sub>2</sub>, **1**, undergoes a reversible, one-electron oxidation that is readily accomplished chemically by silver perchlorate or silver tetrafluoroborate. The oxidation occurs 0.26 V more readily than oxidation of the  $\mu$ -oxo dimer, (OEP)Fe<sup>III</sup>-O-Fe<sup>III</sup>(OEP), and 0.66 V more readily than the monomeric, *meso*-methoxy-substituted complex, ClFe<sup>III</sup>(OEPOMe). This ease of oxidation is attributed at least in part to the effect of direct overlap between the two tetrapyrrole planes in **1**. The <sup>1</sup>H NMR spectrum of the oxidized cation, **1**<sup>+</sup>, shows a number of features, particularly the variation in line widths for the eight methylene resonances, that are consistent with its formulation as a dimer. The pattern of <sup>1</sup>H NMR resonances and the UV/vis spectrum of **1**<sup>+</sup> indicate that a ligand-based oxidation has occurred but that the ligand hole is delocalized over both macrocycles. The stability of **1**<sup>+</sup> depends upon the availability of axial ligands. For example **1**<sup>+</sup> reacts with bromide ion to form **1** and Fe<sup>III</sup>(OEPO<sup>•</sup>)Br in a stoichiometric fashion.

### Introduction

The initial stage of heme breakdown both in heme oxygenase and in the abiological coupled oxidation process involves the *meso* hydroxylation of the porphyrin to form a *meso*-hydroxy-porphyrin (or the tautomeric equivalent, an oxophlorin).<sup>1-4</sup> An examination of the behavior of iron complexes of such peripherally modified porphyrins is essential if heme degradation is to be understood at the molecular level. We have begun a systematic study of the coordination chemistry of iron complexes of the symmetric synthetic porphyrin *meso*-hydroxyoctaethylporphyrin (or octaethyloxophlorin).<sup>5-12</sup> Upon metalation in an inert atmosphere, this macrocycle forms the unusual dimeric complex {Fe<sup>III</sup>(OEPO)}<sub>2</sub>, **1** (OEPO is the trianion of octaethyl-*meso*-hydroxyporphyrin).<sup>5,13</sup> Although efforts to obtain this

dimer in crystalline form suitable for X-ray crystallography have not yet been fruitful, the related dimeric complex {In<sup>III</sup>(OEPO)}<sub>2</sub> has been studied by single-crystal X-ray diffraction.<sup>8</sup> The results show that it does have the basic geometry that has been proposed for {Fe<sup>III</sup>(OEPO)}<sub>2</sub>, **1**. In neutral dimers of this sort, the macrocyclic ligands are present as trianions with the *meso* oxygen of one acting as a donor to the iron(III) ion that is in the center of the adjacent ligand. Thus this structure is quite different from the  $\mu$ -oxo dimers that are prevalent in iron porphyrin chemistry.<sup>14</sup> Those involve a Fe-O-Fe unit that is not present in **1**. Magnetic susceptibility and <sup>1</sup>H NMR studies have revealed that {Fe<sup>III</sup>(OEPO)}<sub>2</sub> is weakly antiferromagnetic with ( $J = -12 \text{ cm}^{-1}$ ).<sup>13</sup>

Some well-characterized reactions of {Fe<sup>III</sup>(OEPO)}<sub>2</sub> are shown in Scheme 1. Notice that all result in cleavage of the dimeric unit. Treatment of **1** with a variety of protic acids such as hydrogen bromide results in loss of the Fe-O bond, protonation of the oxygen atom, and addition of an anionic axial ligand (bromide) to form **2**, BrFe<sup>III</sup>(OEPOH).<sup>5</sup> Addition of excess pyridine to **1** also breaks the dimer with the formation of the bis(pyridine) adduct **3**.<sup>6</sup> Upon oxidation with molecular bromine or chlorine (X<sub>2</sub>), **1** undergoes ligand-centered oxidation to form first **4**, {XFe<sup>III</sup>(OEPO<sup>•</sup>)}, in which the ligand has undergone a one-electron oxidation and is present as a coordinated radical.<sup>7</sup> Further addition of bromine or chlorine produces the six-coordinate complex {X<sub>2</sub>Fe<sup>III</sup>(OEPOx)} in which the tetrapyrrole has undergone two-electron oxidation and is present as a monoanion.<sup>7</sup> The study of such oxidative chemistry is of particular relevance to heme degradation since this is an oxidative process that eventually results in oxidation of the *meso* carbon to carbon monoxide. Clearly, however, the reactions that transform **1** into **4** and **5** occur without the release carbon monoxide.

Here we report that **1** also can undergo a one-electron oxidation which leaves the dimeric unit intact. For this work we have relied extensively on <sup>1</sup>H NMR studies of these

<sup>†</sup> University of California.

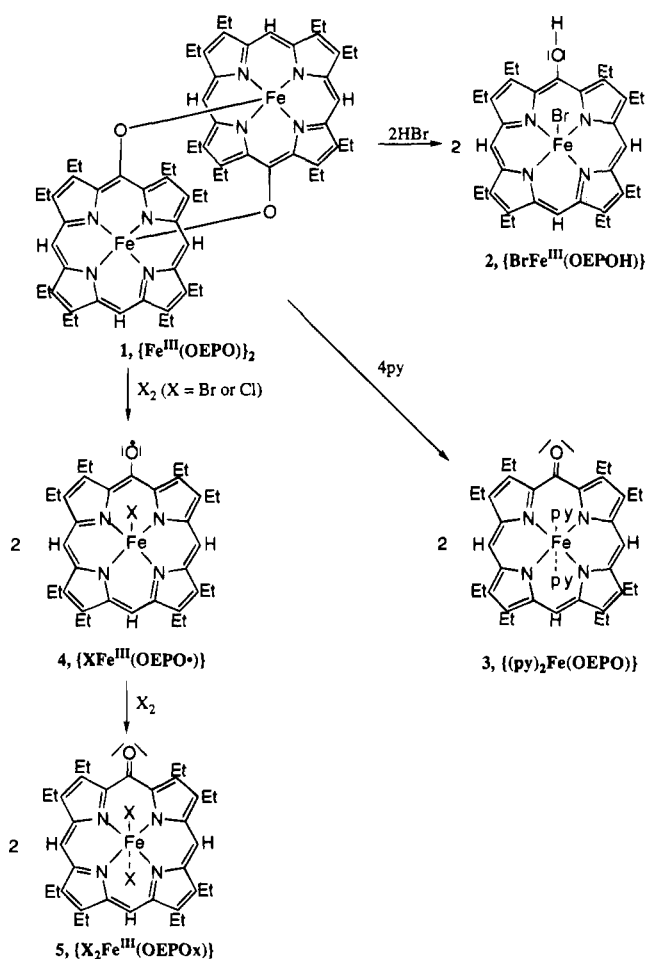
<sup>‡</sup> University of Wrocław.

<sup>®</sup> Abstract published in *Advance ACS Abstracts*, February 15, 1995.

- (1) O'Carra, P. In *Porphyrins and Metalloporphyrins*; Smith, K. M., Ed.; Elsevier: New York, 1975; p 123.
- (2) Schmid, R.; McDonagh, A. F. In *The Porphyrins*; Dolphin, D., Ed.; Academic Press: New York, 1979; Vol. 6, p 258.
- (3) Brown, S. B. In *Bilirubin*; Heirwegh, K. P. M., Brown, S. B., Eds.; CRC Press: Boca Raton, FL, 1982; Vol. 2, p 1.
- (4) Bissell, D. M. In *Liver: Normal Function and Disease. Vol. 4, Bile Pigments and Jaundice*; Ostrow, J. D., Ed.; Marcel Dekker: New York, 1986; p 133.
- (5) Balch, A. L.; Latos-Grażyński, L.; Noll, B. C.; Olmstead, M. M.; Zovinka, E. P. *Inorg. Chem.* **1992**, *31*, 2248.
- (6) Balch, A. L.; Noll, B. C.; Reid, S. M.; Zovinka, E. P. *Inorg. Chem.* **1993**, *32*, 2610.
- (7) Balch, A. L.; Latos-Grażyński, L.; Noll, B. C.; Sztrenberg, L.; Zovinka, E. P. *J. Am. Chem. Soc.* **1993**, *115*, 11846.
- (8) Balch, A. L.; Noll, B. C.; Olmstead, M. M.; Reid, S. M. *J. Chem. Soc., Chem. Commun.* **1993**, 1088.
- (9) Balch, A. L.; Noll, B. C.; Zovinka, E. P. *J. Am. Chem. Soc.* **1992**, *114*, 3380.
- (10) Balch, A. L.; Noll, B. C.; Reid, S. M.; Zovinka, E. P. *J. Am. Chem. Soc.* **1993**, *115*, 2531.
- (11) Balch, A. L.; Noll, B. C.; Phillips, S. L.; Reid, S. M.; Zovinka, E. P. *Inorg. Chem.* **1993**, *32*, 4730.
- (12) Balch, A. L.; Mazzanti, M.; Olmstead, M. M. *Inorg. Chem.* **1993**, *32*, 4737.
- (13) Masuoka, N.; Itano, M. A. *Biochemistry* **1987**, *26*, 3672.

(14) Murray, K. S. *Coord. Chem. Rev.* **1974**, *12*, 1.

Scheme 1



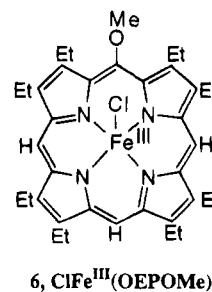
paramagnetic and antiferromagnetic complexes. The  $^1\text{H}$  NMR spectrum of **1** has been thoroughly analyzed.<sup>5</sup> Because of the presence of two iron centers, its spectrum shows a number of notable features. The most striking of these is the variation in line widths of the methylene protons. These spectroscopic features facilitate the identification of both **1** and its one-electron oxidation product,  $\mathbf{1}^+$ .

The ability of **1** to undergo oxidative electron-transfer reactions is of interest in regard not only to the problem of heme catabolism but also to the chlorophyll special pair that occurs in the reaction centers of photosynthetic bacteria.<sup>15–17</sup> These two bacteriochlorophyll molecules are spaced by *ca.* 3.3 Å and make extensive  $\pi$ - $\pi$  contact with one another. A number of synthetic complexes (including bis(porphyrin) sandwich complexes of  $\text{Th}^{\text{IV}}$  and  $\text{Zr}^{\text{IV}}$ <sup>18–20</sup> and unbridged, partially oxidized porphyrin dimers of nickel or copper<sup>21</sup>) have been proposed as models for the unusual electronic interaction between such closely spaced aromatic macrocycles. The iron(III) dimer **1** represents another example of a complex in which the enforced

proximity of two porphyrin-like macrocycles facilitates electron transfer and electron delocalization.

## Results

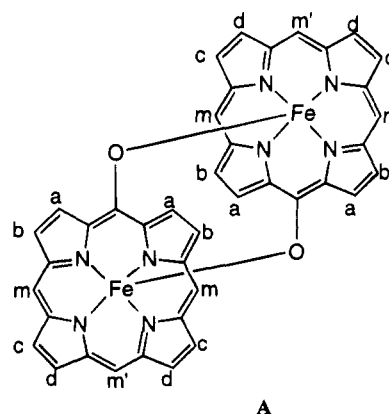
**Electrochemical Studies.** Electrochemical oxidation of  $\{\text{Fe}^{\text{III}}(\text{OEPO})\}_2$  in dichloromethane solution with 0.1 M tetrabutylammonium perchlorate as supporting electrolyte shows a reversible oxidation at 0.13 V vs a silver/silver chloride electrode. This is followed by a second, irreversible oxidation at 0.80 V. For comparison, the first, one-electron oxidation of the  $\mu$ -oxo dimer  $(\text{OEP})\text{Fe}^{\text{III}}\text{OFe}^{\text{III}}(\text{OEP})$  occurs at 0.39 V and the second oxidation at 0.76 V. As a model for a monomeric analog of **1**, the oxidation of the meso-methoxy complex  $\text{ClFe}^{\text{III}}(\text{OEPOMe})$ , **6**, has also been examined. **6** undergoes two



oxidations at 0.79 and 1.10 V and thus is considerably more difficult to oxidize than **1**. In this solvent system, the reversible, one-electron oxidation of ferrocene occurred at 0.37 V.

**Oxidation of  $\{\text{Fe}^{\text{III}}(\text{OEPO})\}_2$ , **1**, with Silver(I) Perchlorate or Silver(I) Tetrafluoroborate.** The oxidation of **1** in chloroform solution with both of these oxidants has been monitored by  $^1\text{H}$  NMR spectroscopy, and in both cases very similar results have been obtained. Figure 1 shows relevant spectra from the reaction between **1** and an acetonitrile- $d_3$  solution of silver(I) perchlorate. The data are presented so that the methylene and meso resonances, which show large hyperfine shifts, are visible. The methyl resonances, which occur in the +10 to -10 ppm region have been cut off so that the others can be seen more readily.

Trace A shows the spectrum of **1**,  $\{\text{Fe}^{\text{III}}(\text{OEPO})\}_2$ , alone. The two meso proton resonances are shifted upfield, while the methylene proton resonances occur in the 40–18 ppm region. The dimeric structure, shown as **A**, requires that there are two



types of meso protons and four types of methylene groups, a–d. Within each of these methylene groups, the two protons are inequivalent. Consequently there are eight methylene resonances. The inset  $\text{A}'$  of Figure 1 shows an expansion of the methylene resonances and emphasizes the location of the two broadest resonances, a and a'. There is a marked variation in

- (15) Diesenhofer, J.; Epp, G.; Miki, K.; Huber, R.; Michel, H. *J. Mol. Biol.* **1984**, *180*, 385.
- (16) Parsons, W. W. In *Photosynthesis*; Ames, J., Ed.; Elsevier: Amsterdam, 1987; p 43.
- (17) Budil, D.; Gast, P.; Chang, C. H.; Schifer, M.; Norris, J. R. *Annu. Rev. Phys. Chem.* **1987**, *38*, 561.
- (18) Buchler, J. W.; Scharbert, B. *J. Am. Chem. Soc.* **1988**, *110*, 4272.
- (19) Bilsel, O.; Rodriguez, J.; Milam, S. N.; Gorlin, P. A.; Girolami, G. S.; Suslick, K. S.; Holten, D. *J. Am. Chem. Soc.* **1992**, *114*, 6528.
- (20) Girolami, G. S.; Gorlin, P. A.; Suslick, K. S. *Inorg. Chem.* **1994**, *33*, 626.
- (21) Scheidt, W. R.; Cheng, B.; Haller, K. J.; Mislankar, A.; Rae, A. D.; Reddy, K. V.; Song, H.; Orosz, R. D.; Reed, C. A.; Cukiernik, F.; Marchon, J.-C. *J. Am. Chem. Soc.* **1993**, *115*, 1181.

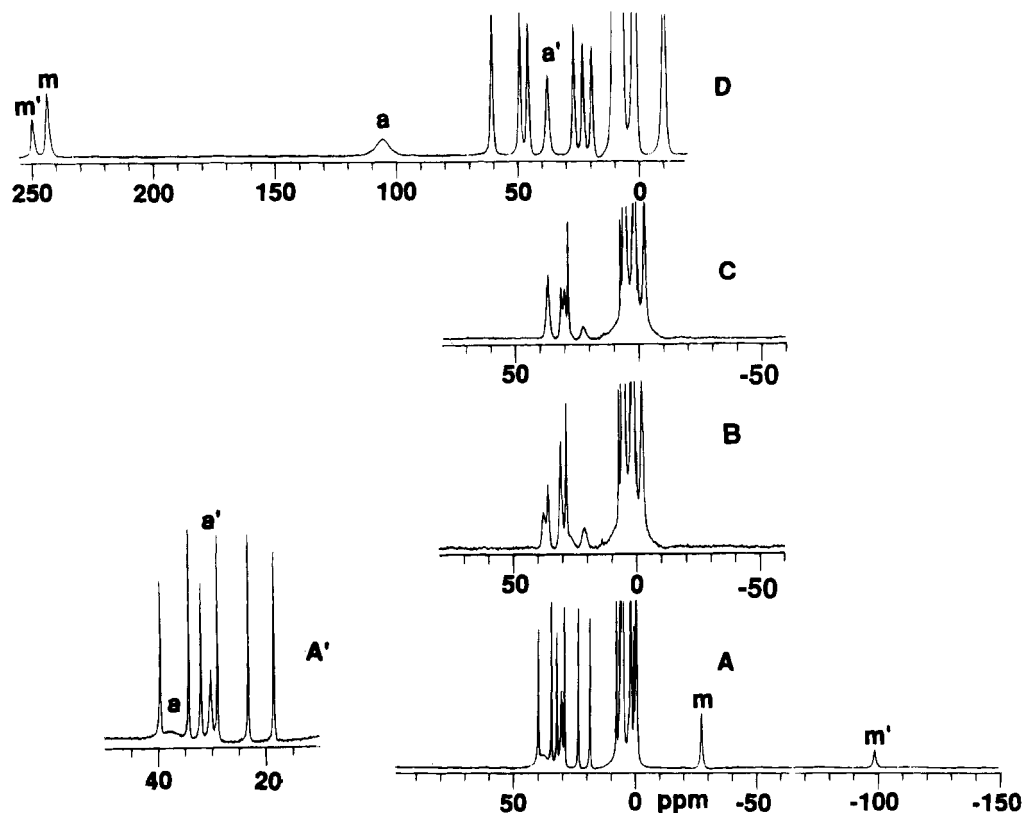


**Figure 1.** 300 MHz  $^1\text{H}$  NMR spectra of the reaction of  $\{\text{Fe}^{\text{III}}(\text{OEPO})\}_2$  in chloroform- $d$ , with  $\text{Ag}^+(\text{ClO}_4)$  in acetonitrile at 25 °C: trace A,  $\{\text{Fe}^{\text{III}}(\text{OEPO})\}_2$  alone with inset A' showing an expansion of the methylene region; trace B, after the addition of 0.50 molar equiv of  $\text{Ag}^+(\text{ClO}_4)$ ; trace C, after the addition of 0.75 molar equiv of  $\text{Ag}^+(\text{ClO}_4)$ ; trace D, after the addition of 1.00 molar equiv of  $\text{Ag}^+(\text{ClO}_4)$ .

$T_1$  values, line widths, and, hence, peak heights of these methylene resonances.<sup>5</sup> The two broadest resonances, those labeled a and a', have been assigned to the two protons of methylene group a. Because of the proximity of this methylene group to the iron ion in the adjacent macrocycle, its protons are most strongly affected by dipolar relaxation from that paramagnetic center. Consequently, these protons are selectively broadened.

Trace B shows the sample after the addition of 0.50 molar equiv of silver perchlorate. All of the methylene resonances have broadened and shifted while the meso resonances are so broad that they cannot be detected. Addition of a total of 0.75 molar equiv of silver(I) perchlorate produces the spectrum shown in trace C. Addition of a total of 1.00 molar equiv of silver(I) perchlorate produces the spectrum shown in trace D. At this point, two meso resonances, at 250 and 243 ppm, in a 1:2 intensity ratio are clearly resolved. Addition of further silver(I) perchlorate does not alter the spectrum. Thus the reaction occurs according to eq 1. During this reaction a black precipitate of silver metal forms as eq 1 requires.

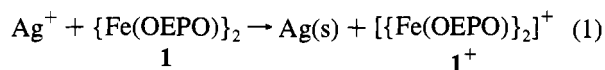
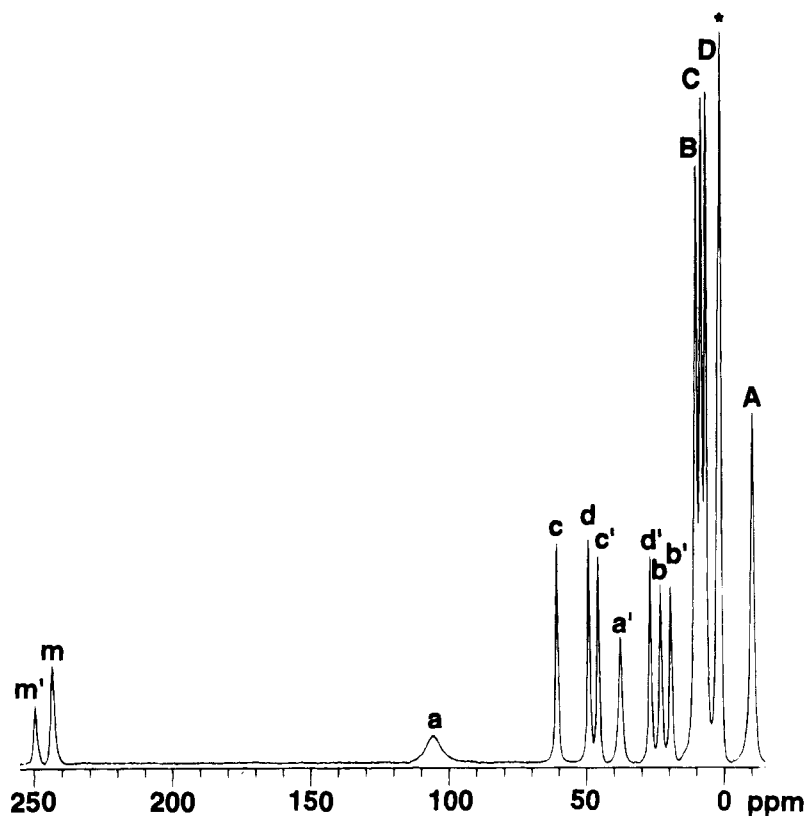


Figure 2 shows the spectrum of  $\{\{\text{Fe}(\text{OEPO})\}_2\}^+$ ,  $1^+$ , so that all resonances can be seen. In addition to the far downfield meso protons and the eight methylene resonances in the 110–20 ppm region, there are four methyl resonances in the +12 to –10 ppm range. All of these resonances have the appropriate integrated intensities, which has facilitated their assignment. The assignment of resonances has been further substantiated by a two-dimensional magnitude COSY (MCOSY) measurement. This type of measurement has been shown to be effective in establishing the connectivity of protons within ethyl groups of

molecules of this sort.<sup>5,22</sup> For the spectrum shown in Figure 2, three cross peaks have been found which connect the methylene resonances b and b' and methyl resonance B, and these then are assigned to a specific ethyl group. Similarly three cross peaks connect resonances c, c', and C of another ethyl group, and another three cross peaks connect resonances d, d', and D for a third ethyl group. By default, resonances a, a', and A belong to the fourth ethyl group. For these, probably because of their greater line widths, we were unable to detect the appropriate cross peaks. A similar situation pertains for  $\{\text{Fe}^{\text{III}}(\text{OEPO})\}_2$ , where the cross peaks for the broadest ethyl group resonances were not observable.<sup>5</sup>

As with  $\{\text{Fe}^{\text{III}}(\text{OEPO})\}_2$ , **1**, there is a significant variation of line widths for the methyl and methylene resonances of  $1^+$ . Within the set of eight methylene resonances, there is one that is extremely broad (at 105 ppm) and a second (at 38 ppm) that is notably broader than the others. Of the four methyl resonances, the one at –10 ppm is also markedly broader than the rest. In order to assess the cause of these variations,  $T_1$  data for all of the resonances have been obtained. The results for a dioxygen-free chloroform- $d$  solution at 25 °C are as follows (in ms). Methylene protons: a, 0.02; a', 0.8; b, 4.0; b', 3.9; c, 7.2; c', 6.1; d, 8.3; d', 8.5. Methyl protons: A, 1.3; B, 6.6; C, 10.5; D, 12.0. Meso protons: m, 1.5; m', 0.8. The  $T_1$  values of the pairs of protons that have been identified by the MCOSY experiment as belonging to a common methylene group have similar magnitudes. These  $T_1$  values can be used to correlate individual resonances with specific locations within the dimeric complex. The dipolar contribution to  $T_1$  is proportional to  $r^{-6}$  where  $r$  is the distance from a specific proton to the iron ion. The paramagnetism of the iron ion attached to the meso-oxygen atom will effect the relaxation of the protons in the ethyl group

(22) Keating, K. A.; deRopp, J. S.; LaMar, G. N.; Balch, A. L.; Shiau, F. Y.; Smith, K. M. *Inorg. Chem.* **1991**, *30*, 3258.



**Figure 2.** 300 MHz  $^1\text{H}$  NMR spectrum of  $[\{\text{Fe}(\text{OEPO})\}_2]^+$ ,  $1^+$ , in chloroform- $d$  solution at 25  $^\circ\text{C}$ . Resonance assignments are made in accord with structure **A** for the dimer. Methylene resonances are identified by lower case letters a–d' while methyl resonances have been denoted by capital letters A–D. Cross peaks in the MCOSEY spectrum (which is not shown) connect resonances into ethyl groups as follows: b, b', and B; c, c', and C; d, d', and D.

(a) that is closest to it and make their resonances the broadest. Thus qualitatively, the  $T_1$  values should increase and line widths decrease in the series of ethyl groups:  $a < b < c < d$ . This allows a complete assignment of all methyl and methylene resonances to the four individual ethyl groups. Similar considerations hold for the methyl resonances, and as expected, methyl group A, which is closest to the iron ion in the adjacent ligand, has the smallest  $T_1$  value and the greatest line width.

The pattern of chemical shifts for the methyl resonances of  $1^+$  (and also of **1** itself) is consistent with a dimeric structure. For  $1^+$ , as seen in Figure 2, one methyl resonance, A, is shifted upfield while the other three have downfield shifts. A similar situation occurs in **1** as well. Since these methyl groups are insulated from the ligand  $\pi$ -system and contact shifts, their chemical shifts will be determined primarily by dipolar effects. Since all methyl groups are nearly equidistant from the iron at the center of the macrocycle to which they are attached, all should experience a similar dipolar shift from that paramagnetic center. However, one methyl group, A, which lies closest to the iron center of the adjacent macrocycle, will experience a larger dipolar shift because of its proximity to that paramagnetic center.

The effects of temperature on the  $^1\text{H}$  NMR spectrum of  $1^+$  are shown in Figure 3, where the chemical shifts are plotted versus  $1/T$ . These plots are not linear as would be expected according to the Curie law for a simple paramagnetic complex. Rather, they show a slight curvature. Monomeric iron(III) porphyrin complexes show some curvature but in the direction opposite to that seen in Figure 3. The curvature in Figure 3 can be ascribed to the effects of antiferromagnetic coupling that may be similar to that between the two iron(III) centers that produces related effects in the spectrum of  $\{\text{Fe}^{\text{III}}(\text{OEPO})\}_2$  itself. However, the situation in  $1^+$  is substantially more complex in

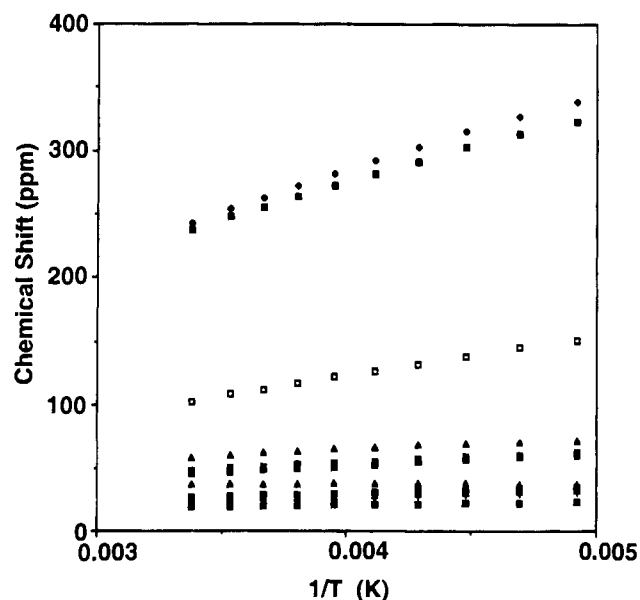


**Figure 3.** Curie plot of the chemical shifts of the meso and methylene resonances of  $[\{\text{Fe}(\text{OEPO})\}_2]^+$  as a function of  $1/T$ .

that three magnetic centers, two Fe iron ions and the ligand radical, are involved.

The magnetic moment of  $1^+$  as measured by the Evans technique<sup>23</sup> for a dichloromethane solution of the complex is  $3.8(2) \mu_B$  per iron atom. This value is lower than that reported for **1** itself ( $4.8 \mu_B$  per iron atom). Consequently it appears that the radical spin in the oxidized dimer  $1^+$  is antiferromagnetically coupled to the iron spins. Additionally the coupling

(23) Evans, D. F. *J. Chem. Soc.* **1959**, 2003.

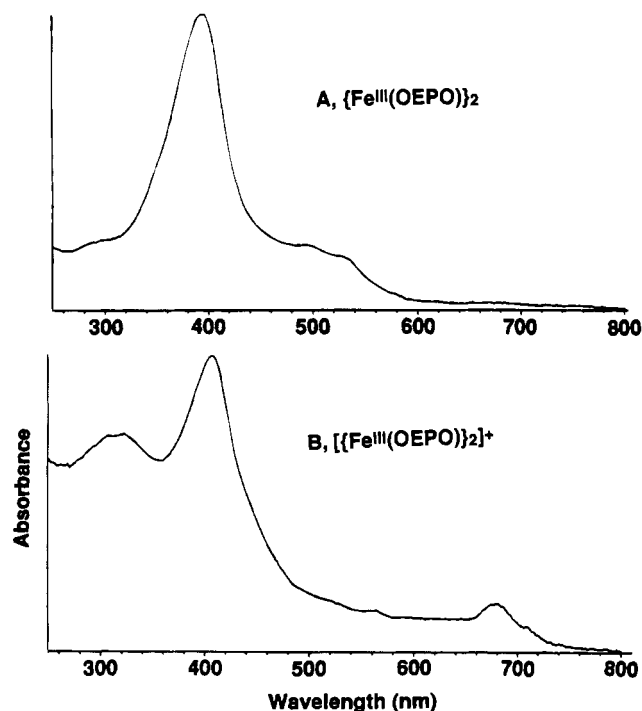
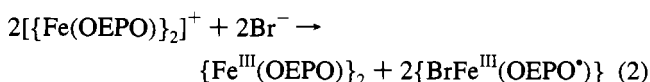


**Figure 4.** The UV/vis absorption spectra of chloroform solutions of (A)  $\{\text{Fe}^{\text{III}}(\text{OEPO})\}_2$ , **1**, and (B)  $[\{\text{Fe}(\text{OEPO})\}_2]^+$ , **1**<sup>+</sup>, generated by  $\text{Ag}^{\text{I}}\text{-ClO}_4$  oxidation of **1**. For **1**<sup>+</sup>,  $\lambda_{\text{max}}$ , nm ( $\epsilon$ ,  $\text{cm}^{-1}\text{M}^{-1}$ ): 396 ( $7.8 \times 10^4$ ), 560 ( $8.2 \times 10^3$ ), 678 ( $1.3 \times 10^4$ ).

between the two iron centers may be perturbed by the oxidation, and further speculation on the interactions between the three paramagnetic centers is unwarranted at this time.

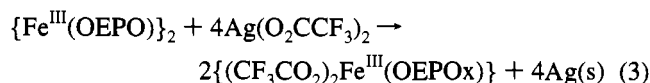
Attempts to isolate **1**<sup>+</sup> from solutions that have been oxidized by silver(I) perchlorate or silver(I) tetrafluoroborate have not been successful. Facile reduction to re-form  $\{\text{Fe}^{\text{III}}(\text{OEPO})\}_2$  appears to be a problem. However, it has been possible to obtain the electronic absorption spectrum of **1**<sup>+</sup> from the oxidized solution. Figure 4 shows a comparison of the absorption spectra of **1** and **1**<sup>+</sup>. Oxidation results in a shift of the Soret band to lower energies and the development of a new band at 678 nm. These spectral features are consistent with ligand-based oxidation and correlate well with the absorption spectrum of **4**,  $\{\text{BrFe}^{\text{III}}(\text{OEPO}^*)\}$ , which has its Soret band at 406 nm and a characteristic low-energy band at 683 nm.

The reaction of **1**<sup>+</sup> with the bromide ion has been examined. Addition of 1 molar equiv of tetra-*n*-butylammonium bromide to a solution of **1**<sup>+</sup> that was prepared from **1** and silver(I) perchlorate produces the <sup>1</sup>H NMR spectrum shown in Figure 5. Comparison of this spectrum with trace A of Figure 1 shows that all of the resonances due to  $\{\text{Fe}^{\text{III}}(\text{OEPO})\}_2$  are present. The remaining resonances are those of  $\text{BrFe}^{\text{III}}(\text{OEPO}^*)$ , **4**.<sup>9</sup> Integration of the spectrum shows that these two species are formed in a 1:2 ratio. The reaction that occurs is shown in eq 2. Since well-resolved spectra are seen for both **1** and **4**, the exchange of ligands and electrons between these two species is slow on the NMR time scale.



**Oxidation of  $\{\text{Fe}^{\text{III}}(\text{OEPO})\}_2$ , **1**, with Silver(I) Trifluoroacetate.** The oxidation of **1** with silver(I) trifluoroacetate takes a course different from that described in the preceding section. Figure 6 shows relevant data. Trace A shows the spectrum of **1** after the addition of 0.25 molar equiv of silver(I) trifluoroac-

etate. Comparison with traces A and B in Figure 1 reveals the following aspects. The resonances of **1** are slightly broadened and shifted. These changes are consistent with what would be expected for the formation of a small quantity of **1**<sup>+</sup>. New resonances are readily apparent in both the downfield and upfield regions. These have no counterparts in the spectra in Figure 1. However they are very similar to the resonances found for  $\text{BrFe}^{\text{III}}(\text{OEPO}^*)$ . Thus there are two meso resonances that have large, downfield hyperfine shifts and there are four resonances in the 58–66 ppm region that can be assigned to the methylene protons. Additionally four resonances appear in the 0 to –15 ppm region that can also be assigned, on the basis of their integrated intensities, to methylene protons. On the basis of the similarity in patterns of resonances, we ascribe these new features in the <sup>1</sup>H NMR spectrum to the formation of the five-coordinate complex  $\{(\text{CF}_3\text{CO}_2)\text{Fe}^{\text{III}}(\text{OEPO}^*)\}$ , **7**. Addition of further quantities of silver(I) trifluoroacetate produces further changes until a total of 4 molar equiv of the oxidant has been added. At that point the spectrum shown in trace B of Figure 6 is obtained. Addition of further quantities of silver trifluoroacetate to the solution does not produce any other changes in the <sup>1</sup>H NMR spectrum. The pattern of resonances seen in trace B resembles the pattern reported for  $\{\text{Br}_2\text{Fe}^{\text{III}}(\text{OEPOx})\}$ .<sup>9</sup> Thus there are three resonances in the 50–30 ppm region with the integrated intensity of the middle resonance twice that of the other two. These are assigned as methylene resonances. Two broader resonances at 19.2 and 29.5 ppm are assigned to the *m'* and *m* protons. Additionally, the EPR spectrum of a dichloromethane solution of **1**<sup>+</sup> (frozen at 9 K) shows an axial spectrum with *g* values of 6.0 and 2.0. Such a spectrum is typical of high-spin ( $S = 5/2$ ) iron(III) complexes, and  $\{\text{Br}_2\text{Fe}^{\text{III}}(\text{OEPOx})\}$  exhibits such a spectrum. These data are consistent with the formation of a six-coordinate complex,  $\{(\text{CF}_3\text{CO}_2)_2\text{Fe}(\text{OEPOx})\}$ , **8**, as shown in eq 3.



## Discussion

The spectroscopic data reported here indicate that  $\{\text{Fe}^{\text{III}}(\text{OEPO})\}_2$ , **1**, can undergo reversible one-electron oxidation without disruption of the dimeric unit to form the cation **1**<sup>+</sup>. In solution, electron exchange between **1** and **1**<sup>+</sup> is sufficiently rapid to cause the <sup>1</sup>H NMR spectra of mixtures of the two to show only a single set of resonances. In contrast, exchange between **1** and  $\{\text{BrFe}^{\text{III}}(\text{OEPO}^*)\}$ , **4**, which involves both electron and ligand exchange, is sufficiently slow so that resonances from each component are clearly resolved (as seen in Figure 5). The cation **1**<sup>+</sup> is stable in solution, but attempts to isolate it as a solid have not been fruitful probably because of facile reduction back to **1**.

The <sup>1</sup>H NMR spectral data are particularly informative with regard to both the geometric and electronic structure of **1**<sup>+</sup>. In regard to geometric structure, the observation of eight, rather than four, methylene resonances is consistent with the presence of a five-coordinate structure for the iron. The marked variation in *T*<sub>1</sub> values and line widths for these eight resonances (as seen in Figure 2) is indicative of a dimeric structure with differential relaxation that is affected by the distances between the individual protons and the two paramagnetic iron centers. Related variations in line widths are also seen the methyl resonances where one resonance (that of methyl protons a) is selectively broadened due to its proximity to the iron ion in the adjacent macrocycle.

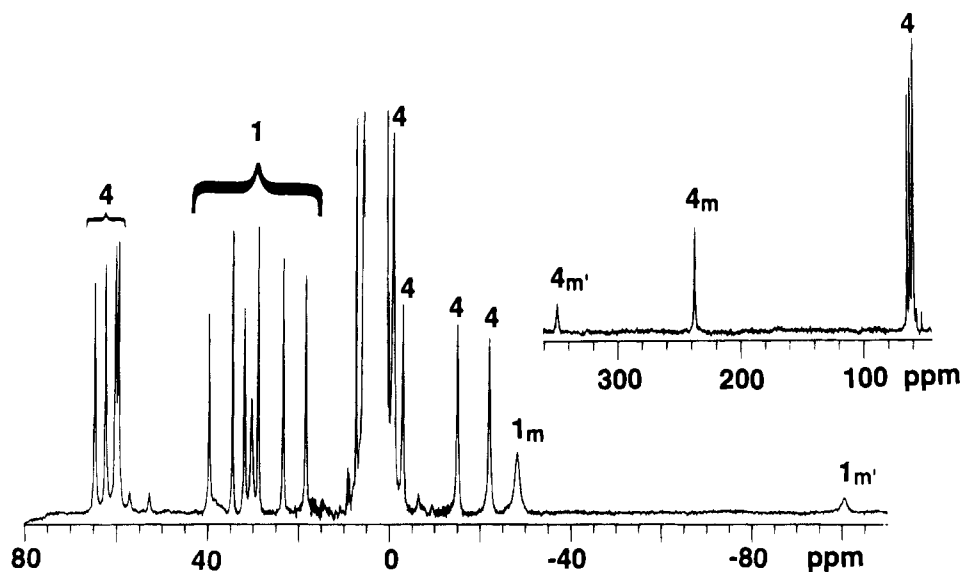


**Figure 5.** 300 MHz  $^1\text{H}$  NMR spectrum of a solution of  $[\{\text{Fe}(\text{OEPO})_2\}(\text{ClO}_4)]$  after treatment with 1.0 molar equiv of tetrabutylammonium bromide. Resonances of  $\{\text{Fe}^{\text{III}}(\text{OEPO})_2\}$ , **1**, and  $\{\text{BrFe}^{\text{III}}(\text{OEPO}^*)\}$ , **4**, are identified by 1 and 4, respectively, with subscripts identifying the meso proton resonances.

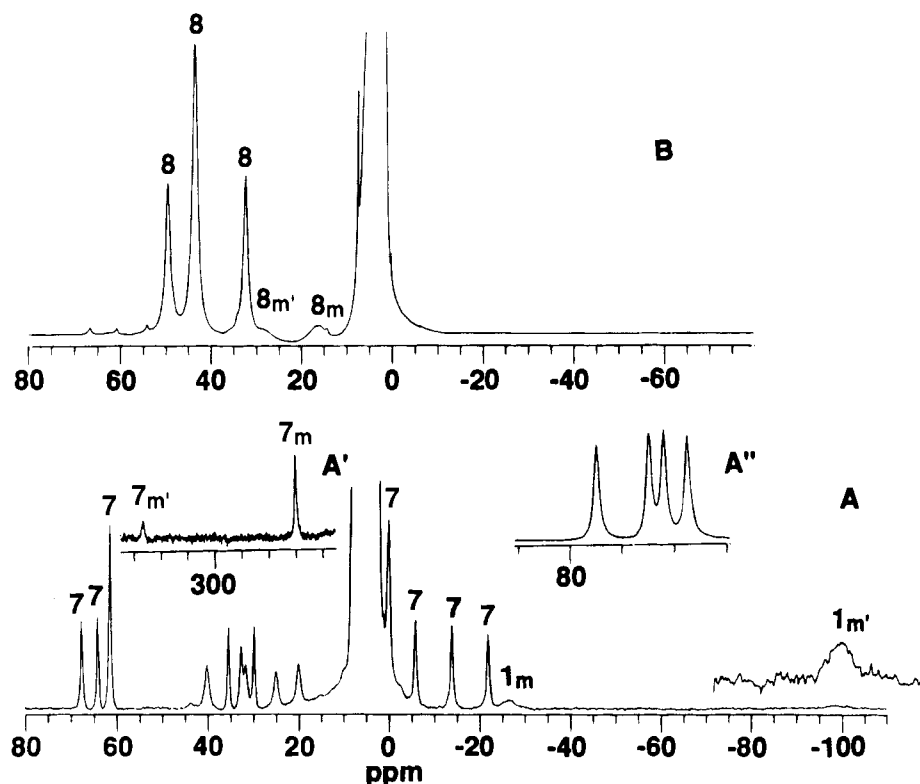


**Figure 6.** 300 MHz  $^1\text{H}$  NMR spectra of the reaction of  $\{\text{Fe}^{\text{III}}(\text{OEPO})_2\}$ , **1**, with  $\text{Ag}(\text{O}_2\text{CCF}_3)$  in acetonitrile- $d_3$  at 23 °C. Trace A is the spectrum after the addition of 0.25 molar equiv of  $\text{Ag}(\text{O}_2\text{CCF}_3)$ . Insert A' shows the region of the spectrum from 360 to 240 ppm. Insert A'' shows the region from 82 to 74 ppm for the sample at -60 °C where the four methylene resonances are clearly resolved. Trace B is the spectrum after the addition of 2.0 molar equiv of  $\text{Ag}(\text{O}_2\text{CCF}_3)$ .

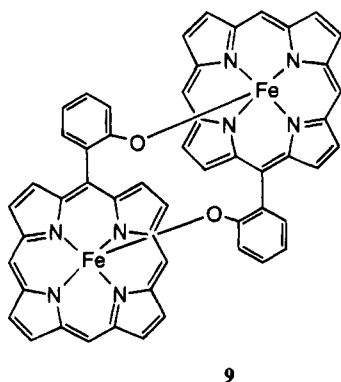
The pattern of resonances from  $\mathbf{1}^+$  is similar in several ways to that of  $\text{BrFe}^{\text{III}}(\text{OEPO}^*)$ , **4**. For both, large, downfield shifts are observed for the meso-hydrogen atoms with the unique m resonance at lowest field. However the magnitude of these hyperfine shifts is smaller for  $\mathbf{1}^+$  than for **4**. For  $\mathbf{1}^+$  and **4**, the methyl resonances are found in the -10 to +10 ppm region. There is some variation in the behaviors of the methylene resonances of the two complexes. Whereas  $\text{BrFe}^{\text{III}}(\text{OEPO}^*)$  has methylene resonances at 70–50 ppm and 0–25 ppm (*i.e.* with both upfield and downfield hyperfine shifts),  $\mathbf{1}^+$  has all of its methylene resonances in the 110–20 ppm region. Additionally,

the electronic spectra of  $\mathbf{1}^+$  and  $\text{BrFe}^{\text{III}}(\text{OEPO}^*)$ , **4**, show features that are consistent with the presence of a ligand-based radical. On the basis of these similarities and the evidence previously described for ligand-based oxidations in the series **1**, **4**, and **5**, we believe that oxidation of **1** results in removal of an electron from one of the tetrapyrrole ligands. This generates a product,  $\mathbf{1}^+$ , which contains two Fe(III) centers, one  $(\text{OEPO})^{3-}$  ligand, and one oxidized  $(\text{OEPO}^*)^{2-}$  ligand. The observation of eight, rather than sixteen, methylene resonances for  $\mathbf{1}^+$  indicates that the two ligands are equivalent. Consequently, the ligand-based unpaired electron must be delocalized over both macrocycles.

As a partial consequence of this delocalization, the hyperfine shifts for the meso resonances of  $1^+$  are smaller in magnitude than those of **4**, in which only one macrocycle is oxidized by one electron.

The extensive delocalization of the ligand hole that is seen for  $1^+$  is of interest in the context of the photosynthetic special pair. The proximity of the two macrocycles appears to facilitate the oxidation of the dimer and allow for extensive delocalization. However, the contribution of the Fe—O linkage in providing a conjugative path for delocalization may also be quite significant. This of course is a problem that is common to all models that use a metal center to hold two tetrapyrrolic units together.<sup>18–20</sup>

A variety of other bridged iron porphyrin dimers have also been seen to undergo one-electron oxidation. The one-electron oxidation of the  $\mu$ -oxo dimer  $\{(\text{OEP})\text{Fe}^{\text{III}}\}_2\text{O}$  occurs 0.26 V more positively than oxidation of **1**.<sup>24,25</sup> The  $^1\text{H}$  NMR spectra of such singly oxidized forms of these iron(III)  $\mu$ -oxo dimers indicate electron delocalization between both porphyrin ligands and rapid electron exchange between the parent  $\mu$ -oxo dimer and its singly oxidized form. The oxidation of **6** occurs 0.56 V more positively than the oxidation of **1**. Complex **6** can be considered as a model for a monomeric iron porphyrin with a meso substituent that approximates the C—O—Fe unit in dimeric **1**. The shift in oxidation potential between **6** and **1** can be attributed to a significant degree to the effect of direct  $\pi$ — $\pi$  overlap on modifying the electronic structure of the dimeric complex. Thus we can conclude that the proximity of the tetrapyrrole planes in **1** significantly facilitates oxidation. Similar conclusions in regard to the effect of the tetrapyrrole ring separation and redox potentials have been made by Buchler and Scharbert.<sup>18</sup> For the phenolate-bridged dimers, **9**, a series



9

of overlapping oxidation waves are seen at 0.55, 0.76, 1.05, and 1.12 V.<sup>26</sup> These are all more difficult oxidations than that seen for **1**. This shift may result from the lower degree of  $\pi$  overlap between the two porphyrins in **9**, where the average perpendicular separation between the porphyrin cores is 4.09 Å. One-electron oxidation of the  $\mu$ -nitrido complex  $\{(\text{TPP})\text{Fe}\}_2\text{N}$  has also been observed.<sup>27</sup>

(24) Goff, H. M.; Phillippi, M. A. *J. Am. Chem. Soc.* **1982**, *104*, 6026.

(25) Arena, F.; Gans, P.; Marchon, J.-C. *Nouv. J. Chim.* **1985**, *9*, 505.

(26) Goff, H. M.; Shimomura, E. T.; Lee, Y. J.; Scheidt, W. R. *Inorg. Chem.* **1984**, *23*, 315.

(27) Kadish, K. M.; Rhodes, R. K.; Bottomly, L. A.; Goff, H. M. *Inorg. Chem.* **1981**, *20*, 3195.

The availability of axial ligands has an important influence on the stability of the dimeric unit in both **1** (as seen in Scheme 1) and  $1^+$ . From the present results it is apparent that perchlorate and tetrafluoroborate are too weakly coordinating to disrupt dimeric  $1^+$ . The results from the titration with silver trifluoroacetate indicate that the trifluoroacetate ion does coordinate and can disrupt dimeric  $1^+$ . Also, addition of bromide ion to  $1^+$  causes the disproportionation given in eq 2 to occur.

## Experimental Section

**Preparation of Compounds.** Octaethylxophlorin and  $\{\text{Fe}^{\text{III}}(\text{OEPO})\}_2$  were prepared as described previously<sup>6,13</sup> except that  $\{\text{Fe}^{\text{III}}(\text{OEPO})\}_2$  was recrystallized from chloroform/methanol before use.  $\text{Ag}^+(\text{ClO}_4)$  and  $\text{Ag}^+(\text{BF}_4)$  were recrystallized from acetonitrile before use.

**$\text{ClFe}^{\text{III}}(\text{OEPOMe)$ , **6**.** A sample of the free base,  $\text{H}_2\text{OEPOMe}$ ,<sup>28</sup> was metalated under standard conditions<sup>6</sup> and purified by chromatography on silica gel with chloroform as eluant.  $^1\text{H}$  NMR in chloroform- $d_1$  (ppm): meso H, -64(2), -76(1); methylene H's, 43.8(1), 43.5(1), 42.2(2), 40.0(1), 38.1(2), 36.4(1). UV/vis in chloroform: 384 (Soret), 510, 540, 640 nm.

**Oxidation of  $\text{Fe}^{\text{III}}(\text{OEPO})\}_2$ , **1**.** Titrations were performed by the addition of aliquots of an 8.8 M solution of  $\text{Ag}^+(\text{ClO}_4)$ ,  $\text{Ag}^+(\text{BF}_4)$ , or  $\text{Ag}^+(\text{O}_2\text{CCF}_3)$  in acetonitrile- $d_3$  by means of a microliter syringe to a solution of  $\{\text{Fe}^{\text{III}}(\text{OEPO})\}_2$  in chloroform- $d$ . The silver metal which formed was removed by filtration through a sintered glass frit.  $\{\text{Fe}^{\text{III}}(\text{OEPO})\}_2$ , **1**, has limited solubility in chloroform or dichloromethane, but the solubility of  $1^+$  generated as the  $\text{ClO}_4^-$  or  $\text{BF}_4^-$  salt is greater. Concentrated solutions of  $1^+$  were obtained by the oxidation of a slurry of  $\{\text{Fe}^{\text{III}}(\text{OEPO})\}_2$  with 1 molar equiv of  $\text{Ag}^+(\text{ClO}_4)$ . The iron complex dissolved as it was oxidized.

**Instrumentation.**  $^1\text{H}$  NMR spectra were recorded on a General Electric QE-300 FT spectrometer operating in the quadrature mode ( $^1\text{H}$  frequency is 300 MHz). The spectra were collected over a 50-kHz bandwidth with 16K data points and a 10- $\mu\text{s}$  90° pulse. For a typical spectrum, between 1000 and 5000 transients were accumulated with a 50-ms delay time. The signal-to-noise ratio was improved by apodization of the free induction decay. The residual  $^1\text{H}$  spectrum of  $\text{CDCl}_3$  or  $\text{CD}_2\text{Cl}_2$  was used as a secondary reference. To obtain unambiguous methyl assignments in the diamagnetic region, an inversion recovery sequence was used with  $\tau$  values varying between 0.2 and 100 ms.

The MCOSEY spectrum<sup>22</sup> was obtained after collecting a standard 1D reference spectrum. The 2D spectrum was collected by use of 512  $t_1$  increments that consisted of 512 scans with a block size of 1024 complex points. A spectral bandwidth of 40 kHz in both dimensions was utilized as the minimum necessary to observe all resonances. A pre-acquisition delay of 150 ms was used. The data were apodized in both dimensions by an unshifted squared sine bell function and zero-filled to form a 1K  $\times$  1K matrix prior to Fourier transformation. A magnitude calculation was performed on the resulting spectrum; this was followed by symmetrization.

Electrochemical measurements were made on a Bioanalytical Systems CV-50W system with a platinum electrode.

**Acknowledgment.** We thank the National Institutes of Health (Grant GM26226) for support, Dr. E. P. Zovinka for experimental assistance with the early stages of this project, and Richard Koerner for the preparation of **6**.

IC941409Q

(28) Evans, B.; Smith, K. M. *Tetrahedron* **1977**, *33*, 629.